Electronic Supplementary Information for

Influence of the framework metal ions on the dye capture behavior of the MIL-100 (Fe, Cr) MOF type solids

Minman Tong,[a] Dahuan Liu,[*a] Qingyuan Yang,[a] Sabine Devautour-Vinot,[b] Guillaume Maurin[b] and Chongli Zhong[a]

[a] State Key Laboratory of Organic-Inorganic Composites, Beijing University of Chemical Technology, Beijing 100029, China

[b] Institut Charles Gerhardt MontpellierUMR CNRS 5253 UM2, UniversitéMontpellier 2, 34095, Montpellier cedex 05, France

E-mail:liudh@mail.buct.edu.cn

1.Experimental and computational details

1.1 Materials

All general reagents and solvents are commercially available and used as received. Iron powder (Fe, ≥ 99%,) and chromium powder (Cr, 99.5%,) were obtained from Aladdin Chemistry Co. Ltd. 1,3,5-benzenetricarboxylic acid (H_3BTC, 99%) was supplied from J&K Scientific Ltd. Nitric acid (HNO_3, 65%~68%), hydrofluoric acid (HF, ≥ 40%), and ethanol (C_2H_5OH, ≥ 99.7%) were purchased from Beijing Chemical Works. Methyl orange ($C_{14}H_{14}N_3NaO_3S$, analytical reagent) and methylene blue ($C_{16}H_{18}ClN_3S$, analytical reagent, ≥ 98.5%) were purchased from Shanghai Maikun Chemical Co. Ltd.

1.2 Preparation of the MOFs

MIL-100(Fe) was synthesized and activated according to the published work. [1] Fe powder (0.82 g), H_3BTC (2.06 g), HF (40%, 0.6 mL), HNO_3 (65%, 1.14 mL), and deionized water (80 mL) were mixed in a Teflon-liner, which was placed in an oven, and was progressively heated to 150 ˚C within 8 hours. The temperature was maintained at 150 ˚C for 4 days and then the oven was cooled down to room temperature in 24 hours. The formed crystals were collected after filtration and then washed with deionized water. The sample was immersed in hot water (80 ˚C) for 3 hours (about 1 g in 300 mL). The as-synthesized MIL-100(Fe) was further purified by keeping in deionized water at 80 ˚C for 5 h to decrease the amount of residual unreacted ions (1 g of sample in 350 mL of water),

and then in hot ethanol at 60˚C for 3 h until no detection of colored impurities in the mother liquor solution, resulting in the highly purified MIL-100(Fe). The solid was finally dried overnight in vacuum at 120˚C.

MIL-100(Cr) was also synthesized and activated according to the literature, [2] using a mixture of metallic chromium (0.52 g), H_3BTC (1.5 g), HF (40%, 4 mL) and deionized water (48 mL). The slurry was introduced in a 125 mL Teflon liner, which was then put into an oven. The system was heated from room temperature up to 220 ˚C in 12 h, and kept at 220 ˚C for 4 days before being cooled to room temperature in 24 h. The resulting light green product was filtered off, washed three times with hot water (reflux), then twice in ethanol (reflux) to remove the excess of unreacted organic ligand and then filtered again. The solid was finally dried overnight in vacuum at 120˚C.

1.3 Characterization of the MOFs

The powder X-ray diffraction (PXRD) patterns were recorded with a Bruker D8 focus diffractometer in reflection mode using Cu Kα radiation. The 2θ range from 5° to 50° was scanned with a step size of 0.02°. Nitrogen physisorption was measured at 77 K on an Autosorb-iQ-MP (Quantachrome Instruments) surface area analyzer. Zeta potentials of the adsorbent in deionized water (20 mg L^{-1}) were measured on a zeta potential analyzer (Malvern Zetasizer, Nano series). The FT-IR spectra of the samples were recorded on a Thermo FT-IR spectrophotometer (Nicolet 6700, USA) using the KBr pellets.

1.4 Dye adsorption/separation on MOFs

A stock solution of 1000 mg L^{-1} MO or MB was prepared by dissolving solid MO or MB in deionized water. Different concentrations of MO or MB solutions were prepared by step-by-step dilution of the stock solution with deionized water. The pH of the MO and MB solution was adjusted with 0.1 M HCl or 0.1 M NaOH. MIL-100(Fe, Cr) were dried overnight at 120˚C before adsorption. To initiate the experiments, 10 mg adsorbent was put into the aqueous dye solutions (50 mL) with fixed initial dye concentrations from 30 ppm to 1000 ppm at 30˚C. After adsorption under magnetic stirring, the solution was separated from the adsorbents with a syringe filter (pore size 0.22 μm). After separation, the solution was analyzed for the concentration of residual MO or MB using a double beam model TU-1901 spectrophotometer (Persee, China) at the calibrated maximum wavelength (max) of 464 nm or 664 nm.

50 mg MIL-100(Fe) or MIL-100(Cr) was added to 10 ml of MO/MB mixture. The initial concentration ratio of the mixed dyes MO and MB ($[MO]_0/[MB]_0$) in solution was set to be 1:1 (50 ppm: 50 ppm). After stirring for 12 h, the concentration of dyes in the solution and the removal of the dyes were determined by UV-Vis spectra.

1.5 Computational methods

Density functional theory (DFT) calculations were performed to evaluate the binding energies between H_2O and the frameworks of MIL-100(Fe, Cr) using Dmol[3] in Materials Studio. [3] Due to the very large number of atoms in a unit cell, the calculations were performed on a Fe_3O/Cr_3O trimer as shown in Fig.S1 by taking Fe_3O as an example. The cleaved bonds of the trimer were saturated by H atoms. The GGA-PBE exchange-correlation functional and DFT semi-core pseudopots core treatment were used with the TS scheme [4] for the dispersion correction for DFT. The double-ξ numerical polarization (DNP) basis set was adopted, which is comparable to the 6-31G(d,p) Gaussian-type basis set.[5]

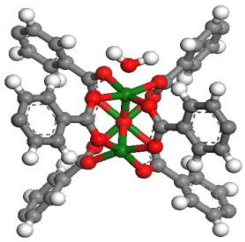

Fig.S1 The Fe_3O trimer in MIL-100(Fe) with one water molecule (Fe, green; O, red; C, gray; H, white).

2. The results of XRD and N_2 physisorption measurements

The as-synthesized MIL-100(Fe, Cr) were characterized by PXRD and N_2 adsorption-desorption experiment. As shown in Fig. S2, the experimental PXRD patterns of the two MOFs are in good agreement with the simulated ones. Both the BET surface area and pore volume for MIL-100(Fe) and MIL-100(Cr) are quite similar (Fig. S3), with 1770 $m^2\ g^{-1}$ vs 1760 $m^2\ g^{-1}$, and 0.76 $cm^3\ g^{-1}$ vs 0.75 $cm^3\ g^{-1}$ respectively, which are close to the previously reported experimental values.[6,7]

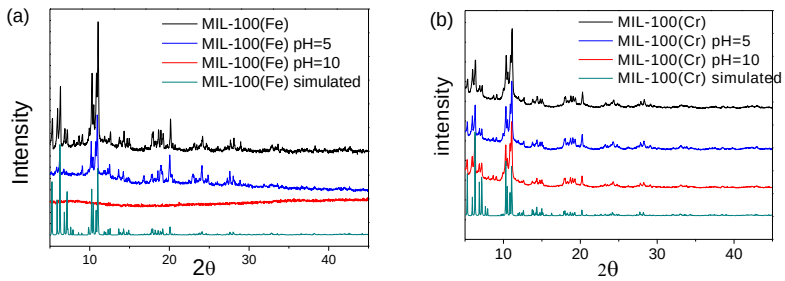

Fig.S2 PXRD patterns of (a) MIL-100(Fe) and MIL-100(Fe) in pH = 5 and pH = 10 MO solutions, (b) MIL-100(Cr) and MIL-100(Cr) in pH = 5 and pH = 10 MO solutions.

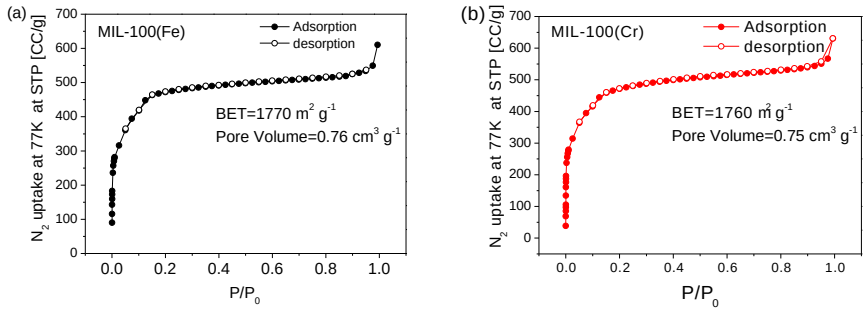

Fig.S3 N_2 adsorption-desorption isotherms of the as-synthesized (a) MIL-100(Fe), (b) MIL-100(Cr).

3. pH effect on MO and MB adsorption

Fig.S4 shows the effect of pH on the adsorption of MO and MB on MIL-100(Fe, Cr). It can be seen that MO is preferentially adsorbed in acid medium on the two MOFs, while MB shows oppositely. In addition, the PXRD patterns (Fig.S2) demonstrated that MIL-100(Fe, Cr) in MO solutions can both maintain their structures when pH = 5. However, when saturated in pH = 10 solutions, the framework of MIL-100(Fe) has already collapsed while MIL-100(Cr) remains unaltered. Based on the above information as well as the stabilities of dye molecules of MO and MB,[8] the pH is therefore set to 5.0 for both dye solutions in the following study.

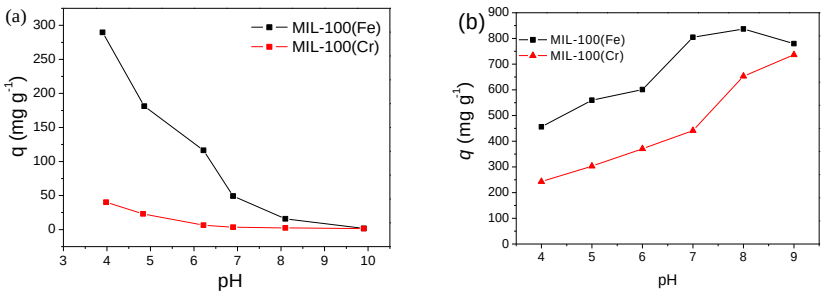

Fig.S4 Effect of pH on the adsorption of (a) MO (100 mg L^{-1}) and (b) MB (200 mg L^{-1}) in MIL-100(Fe, Cr) at 3 days.

4. Comparison with various adsorbents

Table S1 Comparison of the adsorption capacity for MO and MB on various adsorbents

Adsorbents for MO	Adsorption capacity/mg g^{-1}	References
Modified sporopollenin	5.2	9
Activated carbon	9.5	10
Chitosan/Alumina	35.3	11
MIL-53(Cr)	57.9	12
AC/ferrospinel	95.8	13
CNTs-A	149.0	14
Zn/Al-LDO	181.9	15
PED-MIL-101	194.0	12
Activated carbon	238.1	16
Mesoporous carbon	295.4	17
Activated carbon	300.0	18
SBA-3	357.1	19
NH_3^+-MCM-41	366.6	20
PANI/ α-ZrP	377.5	21
PAC-HNO_3	384.6	22
Polyaniline hollow spheres	384.6	23
MOF-235	477.0	24
MPSC/C	637.0	25
Mg_3Al-LDH	1407.5	26
Cu_2O MPS	1424.0	27
MIL-100(Cr)	211.8	This work
MIL-100(Fe)	1045.2	This work
Adsorbents for MB	**Adsorption capacity/mg g^{-1}**	**References**
Marine seaweed	5.2	28
Rice husk	9.8	29
Hierarchically mesostructured MIL-101	21.0	30*
Yellow passionfruit	44.7	31
GFC190	73.26	32
Na-ghassoulite	135.0	33
Graphene sponge	184.0	34
CNTs	190.9	35
BN hollow spheres	191.7	36
MOF-235	252.0	24
Cobalt-hectorite composite	355.0	37
CNTs-A	399.0	14
Bamboo-activated carbon	454.2	38
Waste teaactivated carbon	544.3	39
MPSC/C	758.0	25
Sargassummuticum	860.0	40
CTS-g-PAA/MMT	1859.0	41
MIL-100(Cr)	645.3	This work
MIL-100(Fe)	736.2	This work

*Measurement was carried out only at C_0=30 ppm.

5. The results of FT-IR measurement

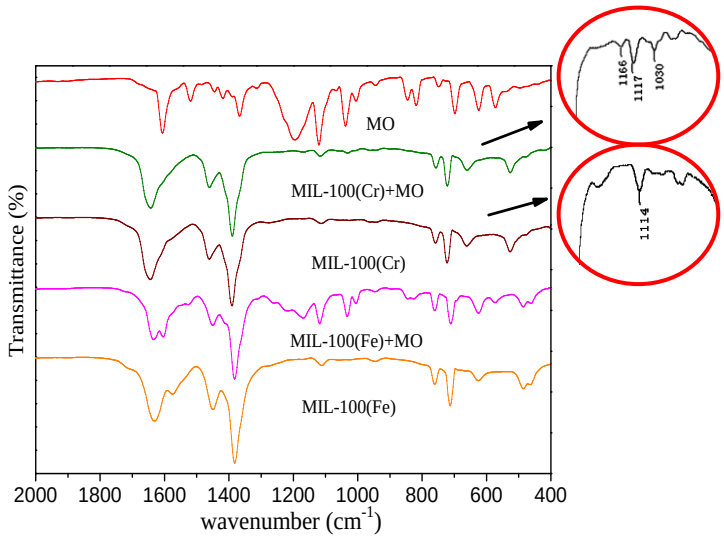

Fig. S5 The FT-IR spectra of MO, MIL-100(Fe, Cr) and MO loaded MIL-100(Fe, Cr).

6. Pseudo-second-order kinetic model

The pseudo-second-order kinetic model [42] successfully described the kinetics of MO and MB adsorption for different initial dye concentrations, as confirmed by good linearity (Fig. S6). The linear form of the equation is:

$$\frac{t}{q_t} = \frac{1}{k_2 q_e^2} + \frac{1}{q_e} t \qquad \text{(Eq. S1)}$$

where, t is the adsorption time (h), q_e and q_t are the amount adsorbed at equilibrium and at time t, respectively (mg g^{-1}), and k_2 is the rate constant for pseudo-second-order adsorption (g mg^{-1} h^{-1}). k_2 = *slope*^{2}/*intercept* when the t/q_t is plotted against t.

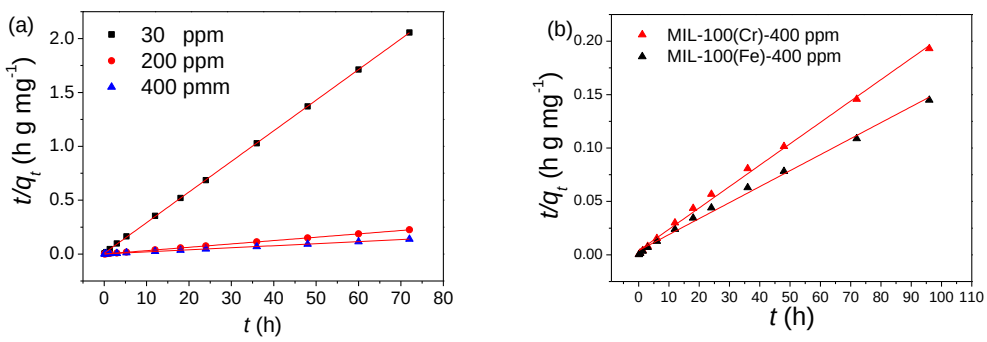

Fig.S6 Plots of pseudo-second-order kinetics for the adsorption of (a) MO on MIL-100(Fe) and (b) MB on MIL-100(Fe, Cr).

Table S2 Kinetic Parameters for the Adsorption of MO, MB on MIL-100(Fe) and MB on MIL-100(Cr) at 30 °C

Adsorbent	Dye	C_0 /ppm	Pseudo-second-order kinetic model			
			q_e(exp)[a] /mg g^{-1}	q_e(cal)[b] /mg g^{-1}	k_2 /g mg^{-1} h^{-1}	R^2
MIL-100(Fe)	MO	30	35.0	35.2	1.107×10^{-1}	1.000
		200	320.1	321.4	1.239×10^{-2}	1.000
		400	540.2	546.1	2.327×10^{-3}	0.999
	MB	400	662.3	666.7	5.613×10^{-4}	0.995
MIL-100(Cr)	MB	400	496.9	499.6	1.028×10^{-3}	0.997

[a] calculated adsorption capacity;

[b] experimental adsorption capacity.

7. Langmuir isotherm model

The form of the Langmuir isotherm [43] was found to fit well the data of MO and MB adsorption isotherms on MIL-100(Cr, Fe) by the following equation:

$$q_e = q_m \frac{K_L C_e}{1 + K_L C_e} \qquad \text{(Eq. S2)}$$

where q_e is the amount of dye adsorbed per gram of adsorbent (mg g^{-1}), C_e denotes the equilibrium concentration of dye in solution (mg L^{-1}); K_L represents the Langmuir constant (L mg^{-1}) that relates to the affinity of binding sites, and q_m is a theoretical limit of adsorption capacity when the monolayer surface is fully covered with dye molecules to assist in the comparison of adsorption performance (mg g^{-1}).

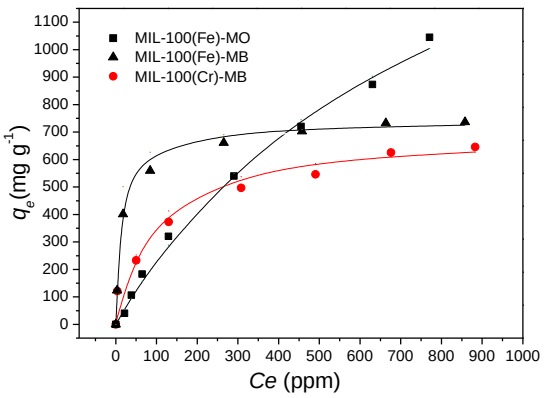

Fig.S7 Adsorption isotherms at 30˚C for MO, MB on MIL-100(Fe) and MB on MIL-100(Cr). Solid lines refer to the fitted adsorption isotherms by the Langmuir equation.

Table S3 Langmuir Constants for the Adsorption of MO, MB on MIL-100(Fe) and MB on MIL-100(Cr)

			Langmuir constants		
Adsorbent	Dye	T/ °C	K_L/ L mg^{-1}	q_m/ mg g^{-1}	R^2
MIL-100(Fe)	MO	30	2.599	2014.9	0.993
	MB	30	0.0409	744.77	0.996
MIL-100(Cr)	MB	30	0.0115	689.65	0.979

8. Zeta potentials of MIL-100(Cr)

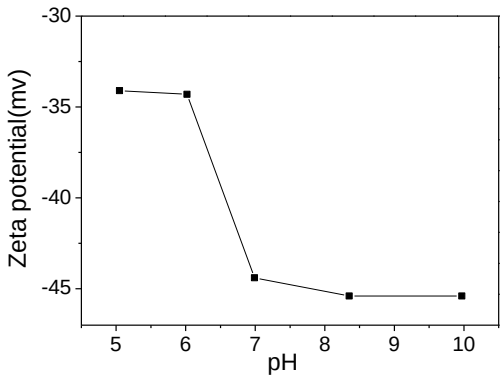

Fig. S8 Effect of pH on the zeta potentials of MIL-100(Cr)

References

1 J. W. Yoon, Y.-K. Seo, Y. K. Hwang, J.-S. Chang, H. Leclerc, S. Wuttke, P. Bazin, A. Vimont, M. Daturi, E. Bloch, P. L. Llewellyn, C. Serre, P. Horcajada, J.-M. Grenèche, A. E. Rodrigues and G. Férey, *Angew. Chem., Int. Ed.*, 2010, **49**, 5949-5952.

2 G. Férey, C. Serre, C. Mellot-Draznieks, F. Millange, S. Surble, J. Dutour and I. Margiolaki, *Angew. Chem., Int. Ed.*, 2004, **43**, 6296-6301.

3 *Materials Studio*, 5.5 V; Accelrys Inc., San Diego, 2010.

4 A. Tkatchenko and M. Scheffler, *Phys. Rev. Lett.*, 2009, **102**, 073005.

5 Y. F. Chen, R. Babarao, S. I. Sandler and J. W. Jiang, *Langmuir*, 2010, **26**, 8743-8750.

6 S.-H. Huo and X.-P. Yan, *J. Mater. Chem.*, 2012, **22**, 7449-7455.

7 L. Hamon, N. Heymans, P. L. Llewellyn, V. Guillerm, A. Ghoufi, S. Vaesen, G. Maurin, C. Serre, G. D. Weireld and G. D. Pirngruber, *Dalton Trans.*, 2012, **41**, 4052−4059.

8 W. Zhang, H. Li, X. Kan, L. Dong, H. Yan, Z. Jiang and H. Yang, *Bioresour. Technol.*, 2012, **117**, 40-47.

9 A. Ayar, O. Gezici and M. Kucukosmanoglu, *J. Hazard. Mater.*, 2007, **146**, 186-193.

10 K. P. Singh, D. Mohan, S. Sinha, G. S. Tondon and D. Gosh, *Ind. Eng. Chem. Res.*, 2003, **42**, 1965-1976.

11 J. Zhang, Q. Zhou and L. Qu, *J. Chem. Eng. Data*, 2012, **57**, 412-419.

12 E. Haque, J. E. Lee, I. T. Jang, Y. K. Hwang, J.-S. Chang, J. Jegal and S. H. Jhung, *J. Hazard. Mater.*, 2010, **181**, 535-542.

13 L. Ai and J. Jiang, *Desalination*, 2010, **262**,134-140.

14 J. Ma, F. Yu, L. Zhou, L. Jin, M. Yang, J. Luan, Y. Tang, H. Fan, Z. Yuan and J. Chen, *ACS Appl. Mater. Interfaces*, 2012, **4**, 5749-5760.

15 Z.-M. Ni, S.-J. Xia, L.-G. Wang, F.-F. Xing and G.-X. Pan, *J. Colloid Interface Sci*., 2007, **316**, 284-291.

16 S. Chen, J. Zhang, C. Zhang, Q.Yue, Y. Li and C. Li, *Desalination*, 2010, **252**, 149-156.

17 N. Mohammadi, H. Khani, V. K. Gupta, E. Amereh and S. Agarwal, *J. Colloid Interface Sci.*, 2011, **362**, 457-462.

18 K. Mahmoudi, N. Hamdi, A. Kriaa and E. Srasra, Russ. *J. Phys. Chem. A*, 2012, **86**, 1294-1300.

19 M. Anbia, S. A. Hariri and S. N. Ashrafizadeh, *Appl. Surf. Sci.*, 2010, **256**, 3228-3233.

20 Q. Qin, J. Ma and K. Liu, *J. Hazard. Mater.*, 2009, **162**, 133-139.

21 L. Wang, X.-L. Wu, W.-H. Xu, X.-J. Huang, J.-H. Liu and A.-W. Xu, *ACS Appl. Mater. Interfaces*, 2012, **4**, 2686-2692.

22 M. H. Do, N. H. Phan, T. D. Nguyen, T. T. S. Pham, V. K. Nguyen, T. T. T. Vu and T. K. P. Nguyen, *Chemosphere*, 2011, **85**, 1269-1276.

23 X. Guo, G. T. Fei, H. Su and L. D. Zhang, *J. Mater. Chem.*, 2011, **21**, 8618-8625.

24 E. Haque, J. W. Jun and S. H. Jhung, *J. Hazard. Mater*., 2011, **185**, 507-511.

25 X. Zhuang, Y. Wan, C. Feng, Y. Shen and D. Zhao, *Chem. Mater.*, 2009, **21**, 706-716.

26 K. Morimoto, K. Tamura, N. Iyi, J. Ye and H. Yamada, *J. Phys. Chem. Solids*, 2011, **72**, 1037-1045.

27 Y. Shang, D. Zhang and L. Guo, *J. Mater. Chem.*, 2012, **22**, 856-861.

28 S. Cengiz and L. Cavas, *Bioresour. Technol*., 2008, **99**, 2357–2363.

29 Y. C. Sharma and Uma, *J. Chem. Eng. Data*, 2010, **55**, 435–439.

30 X.-X. Huang, L.-G. Qiu, W. Zhang, Y.-P. Yuan, X. Jiang, A.-J. Xie, Y.-H. Shen and J.-F. Zhu, *CrystEngComm*, 2012, **14**, 1613-1617.

31 F. A. Pavan, E. C. Lima, S. L. P. Dias and A. C. Mazzocato, *J. Hazard. Mater.*, 2008, **150**, 703–712.

32 W. Fan, W. Gao, C. Zhang, W. W. Tjiu, J. Pan and T. Liu, *J. Mater. Chem.*, 2012, **22**, 25108-25115.

33 Y. E. Mouzdahir, A. Elmchaouri, R. Mahboub, A. Gil and S. A. Korili, *J. Chem. Eng. Data*, 2007, **52**, 1621-1625.

34 J. Zhao, W. Ren and H.-M. Cheng, *J. Mater. Chem.*, 2012, **22**, 20197–20202.

35 Z. Sui, Q. Meng, X. Zhang, R. Mab and B. Cao, *J. Mater. Chem.*, 2012, **22**, 8767–8771.

36 G. Lian, X. Zhang, S. Zhang, D. Liu, D. Cui and Q. Wang, *Energy Environ. Sci.*, 2012, **5**, 7072-7080.

37 J. Ma, Y. Jia, Y. Jing, Y. Yao and J. Sun, *Dyes Pigm.*, 2012, **93**, 1441-1446.

38 B. H. Hameed, A. T. M. Din and A. L. Ahmad, *J. Hazard. Mater.*, 2007, **141**, 819–825.

39 M. Auta and B. H. Hameed, *Chem. Eng. J.*, 2011, **175**, 233–243.

40 E. Rubín, P. Rodríguez, R. Herrero and M. E. S. de Vicente, *J. Chem. Eng. Data*, 2010, **55**, 5707–5714.

41 L. Wang, J. Zhang and A. Wang, *Colloid Surf. A-Physicochem. Eng. Asp.*, 2008, **322**, 47–53.

42 L. Ai, C. Zhang and L. Meng, *J. Chem. Eng. Data*, 2011, **56,** 4217-4225.

43 I. Langmuir, *J. Am. Chem. Soc*. 1918, **40**, 1361-1403.